Proceedings of ICRC 2001: 4011 © Copernicus Gesellschaft 2001

ICRC 2001

Cosmic ray measurements on board space station MIR with SILEYE-2 experiment

M. Casolino[1], V. Bidoli[1], E. De Grandis[1], M. De Pascale[1], G. Furano[1], A. Morselli[1], L. Narici[1], P. Picozza[1], G. Percossi[1], R. Sparvoli[1], E. Reali[1], A. Bakaldin[2], A. Galper[2], S. Koldashov[2], M. Korotkov[2], A. Galper[2], A. Khodarovich[2], M. Korotkov[2], A. Popov[2], N. Vavilov[2], M. Boezio[3], V. Bonvicini[3], A. Vacchi[3], N. Zampa[3], P. Papini[5], P. Spillantini[5], M. Ricci[6], G. Castellini[7], P. Carlson[8], and C. Fuglesang[9]

[1]Univ. of Rome "Tor Vergata" and INFN sezione di Roma2, Rome, Italy
[2]Moscow Engineering Physics Institute, Moscow, Russia
[3]Univ. of Trieste and INFN sezione di Trieste, Trieste, Italy
[5]Univ. of Firenze and INFN sezione di Firenze, Firenze, Italy
[6]INFN Laboratori Nazionali di Frascati, Frascati, Italy
[7]Istituto di Ricerca Onde Elettromagnetiche CNR, Firenze, Italy
[8]Royal Institute of technology, Stockholm, Sweden
[9]European Astronaut Centre, ESA, Cologne, Germany.

Abstract. SilEye-2 is a silicon detector telescope built for the study of the causes of Light Flashes perception by astronauts. As a stand-alone device, it can also monitor the real time radiation composition inside MIR. The device was operational for more than 1000 hours in the years 1998-2000, detecting also several Solar Particle Events. In this work we show the nuclear discrimination capabilities of the device and nuclear abundance data from Boron to Silicon above $\simeq 150$ MeV/n. We also present Linear Energy Transfer measurements inside MIR.

1 Introduction

Studying and understanding the cosmic ray and radiation environment in space is of utmost importance not only for the astrophysical issues related but also for the effects on human physiology and health. Crew safety issues in the construction of the International Space Station (ISS) and a future mission to Mars make this items even more essential. Radiation in orbit comes from cosmic rays of galactic and solar nature. The galactic component is modulated by the 11 year solar cycle at low energies (below 1 GeV) and gives a contribution roughly constant for periods shorter than half of the solar cycle. Transient phenomena of Solar Energetic Particles (SEPs) due to solar flares and coronal mass ejections can however give an unexpected significant contribution to the total particle fluence and dose absorbed by the astronauts, especially if they are outside the geomagnetic shielding. Inside Earth's magnetosphere there is also the contribution of trapped particles, mostly protons. For Low Earth Orbits such as those of MIR, ISS or Shuttle (altitude of 300-400 km, inclination of 51.6^o) the effect of trapped radiation is mostly evident in the South Atlantic Anomaly (SAA). This is a region located between South America and Africa were the geomagnetic field is lower and particle flux increases. For a correct dose measurement it is important to study not only flux but relative nuclear composition for its high quality factor which can give a non-negligible contribution even with a low particle flux.

Besides to the effects due to radiation, there are also other processes that have to be studied in order to have a more complete knowledge of the human response to space environment. One of these phenomena is the "Light Flashes" (LF) effect, originally predicted by Tobias(Tobias, 1952) and reported for the first time in 1969 by the Apollo-11 mission to the Moon. Subsequently, LF were observed by astronauts in the Apollo, Skylab, Shuttle and MIR missions (Malachowski, 1978; Horneck, 1992; McNulty, 1996). The SilEye- 1 and 2 experiments were built to study both this phenomenon and the radiation environment on board space station MIR. For their characteristics, active silicon detectors (Reitz, 1996; Sakaguchi et al., 1999) are particularly suited to cosmic ray and radiation measurements in space. SilEye-1 was operational on MIR between December 1995 and December 1997(Galper et al., 1996). It performed the first LF observations on MIR and carried the prototype of the silicon detector. SilEye-2 was first turned on in February 1998 with systematic observations starting in October 1998. It was operational in various periods until August, the 28^{th}, 1999. When the last crew reached MIR on March 2000, SilEye-2 was turned on again during the mission (until June 2000) (Bidoli et al., 1997, 2000).

In this work we discuss the in-flight performances of the detector and particle composition on board space station MIR using data gathered between August 1998 and August 1999. This data set consists of 93 sessions, 17 of which devoted to Light Flashes observations. More than 10^7 particle events have been acquired in 1068 hours of observation time: during

Correspondence to: Marco.Casolino@roma2.infn.it

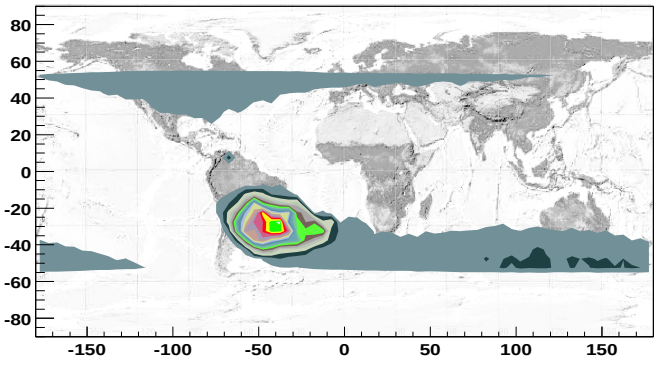

Fig. 1. Acquisition rate as a function of position (Y: latitude - degrees, X: longitude - degrees) for all solar quiet sessions. It is possibile to see the increase in the SAA region. Each contour level represents a flux increase of 3 Hz.

these observations 7 Solar Particle Events (SPEs) were also detected. The latest data set (year 2000) is currently under analysis. LF results are presented in Avdeev et al. (2000).

2 The experimental device

SilEye-2 consists of a silicon detector telescope, housed in an aluminium box, coupled to an "helmet" with an eye mask, and worn by the cosmonaut for Light Flash measurement sessions.

The device can also be operated as a stand-alone cosmic ray detector without the presence of the cosmonaut; in this acquisition mode it is possible to measure in real time the environmental radiation inside MIR.

The particle detector telescope is made of a series of six silicon active layers, originally developed in the construction of NINA-1 and 2 cosmic ray space telescopes Bidoli et al. (2001); Sparvoli et al. (2000). Each of the six silicon wafers has and active area of $60 \times 60\, mm^2$, divided in 16 strips each 3.6 mm wide; the thickness is $380 \pm 15\ \mu m$. Two wafers, orthogonally glued back to back, constitute a plane. Three planes are used together, for a total number of 96 strips and an active thickness of 2.28 mm. The distance between the silicon planes is 14 mm; the geometrical factor is 85 cm^2 sr if particles hitting the detector from both sides are considered.

Two passive absorbers (1 mm iron each) are inserted between the position-sensitive detectors to extend the energy range. Each trigger, data are converted by a 12 bit ADC and sent to a FIFO for acquisition by the read out card. The ADC has a dynamic range up to 12.2 pC of injected charge: thus SilEye-2 can measure particle energy losses per strip from 0.25 MeV ($0.69\, keV/\mu m$) to about 300 MeV ($830\, keV/\mu m$) and then determine nuclear species. The analogic sum of the signals from the strips of each view is used as a input for the trigger system, which requires that particles cross all the detector in order to be read. The trigger threshold is placed at $0.69\ keV/\mu m$. Particles are therefore required to cross the detector in order to have a trigger to read the event. The minimum particle energy - determined with

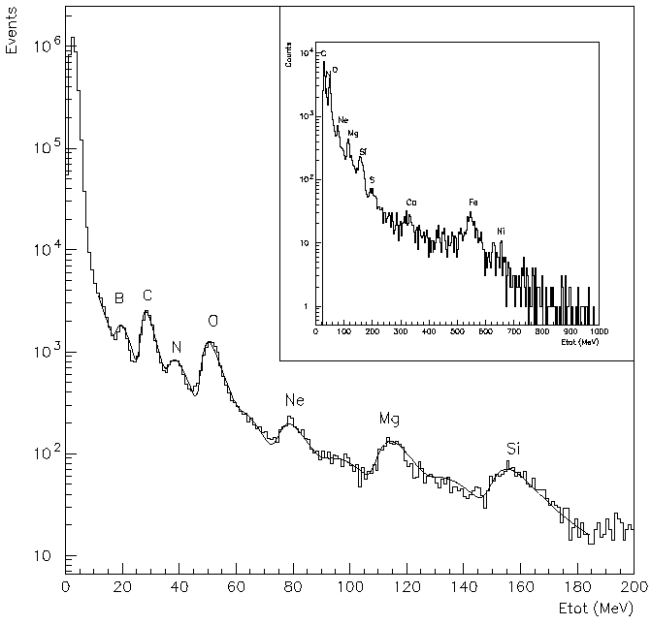

Fig. 2. Nuclear identification capabilities of SilEye-2 for nuclei up to Si. In the inset is shown the contribution of nuclei up to Ni. The continuous line corresponds to a fit using a Landau distribution per nuclear species (see text).

Montecarlo simulations - varies from 30 MeV for H to 80 MeV/n for O to 150 MeV/n for Fe. The 0.69 $keV/\mu m$ trigger threshold, necessary to optimise the detector for high Z nuclei observation (of higher interest for LF), reduces proton detection efficiency at high energies (above 200 MeV). As energy increases the energy deposited decreases and reduces trigger probability (due to fluctuations in the energy loss): above 400 MeV the efficiency is $\simeq 7\%$. Particles from both sides of the detector are read: however the material crossed is different in the two cases, since particles cross the 0.2 mm Cu window on one side (closer to the cosmonaut's head) and $\simeq 2$ cm of electronics on the other. This requires a correction in the energetic spectrum of low energy particles coming from this direction, but - aside from nuclear fragmentation in the interposed material - does not appreciably affect nuclear composition.

3 Nuclear Abundances

The study of the radiation environment on board manned spacecraft requires evaluation of the dose absorbed by the astronauts in order to assess the risks involved in space missions. The complexity of the information required for a detailed comprehension of the radiation environment grew with the improvement of the detectors and the understanding of the near Earth and interplanetary radiation environment. The use of active detectors allows a measurement in real time of the nature of charged radiation impinging on the spacecraft and the modifications of the cosmic ray flux due to the interaction with the material of the spacecraft

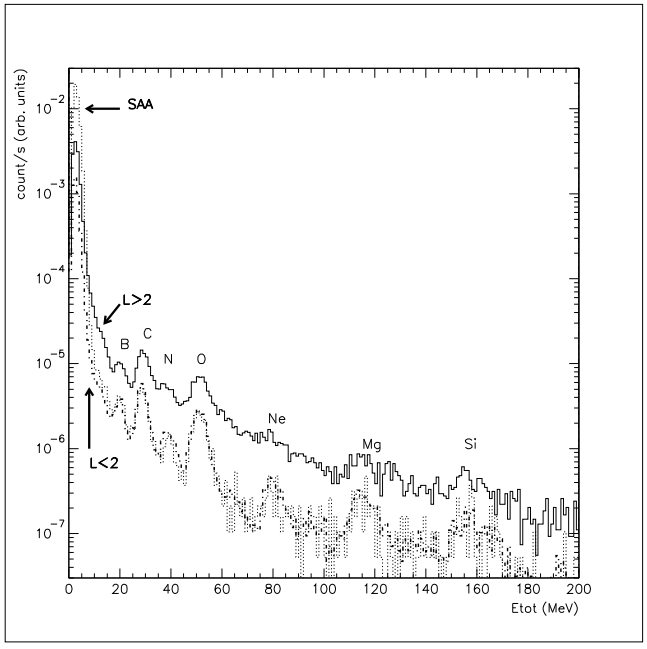

Fig. 3. High energy nuclear abundances: Continuous line: galactic ($L > 2$) component; Dotted line: SAA component ($L < 2,\ B < 0.25G$); Dashed line: remaining region ($L < 2,\ B \geq 0.25G$). Note the equal $Z \geq 5$ abundance for the $L < 2$ zones as compared to galactic component and the different proton abundances.

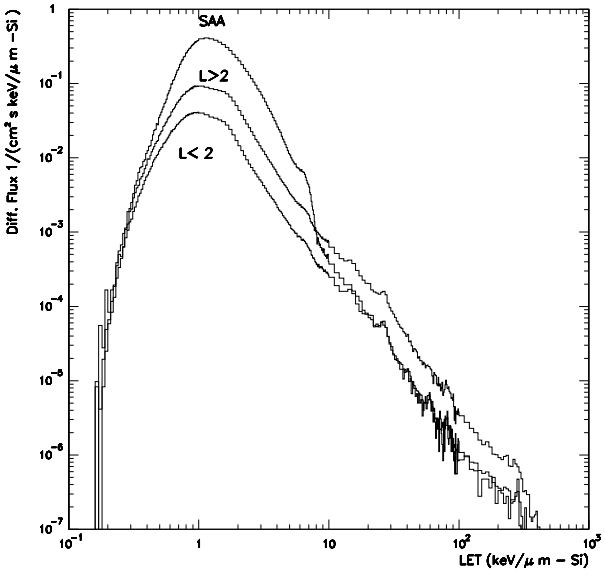

Fig. 4. Linear Energy Transfer in silicon for solar quiet period measured with SilEye-2 (solar quiet sessions between August 1998 and August 1999). Top: SAA region. Center: galactic ($L > 2$) region. Bottom: remaining region ($L < 2$, outside the SAA.

itself. These studies have to be carried forth in solar quiet and active conditions, in order to take into account the contribution to the dose absorbed by astronauts during SEPs. The time and intensity variability of these events make them real threats to long term activities outside the geomagnetic shielding such as a mission to Mars (Spillantini (2000)). The calibration of the device is performed selecting high energy (above 100 MeV) particles crossing the detector. Average energy loss for each nuclear species can be assumed constant with fluctuations described by the Landau distribution. The relation between ADC channel and energy loss is establihed with Geant 3.21 Montecarlo simulation.

SilEye-2 can identify nuclear species up to Fe and therefore measure relative abundances inside MIR in different positions and solar activity conditions. To identify each nuclear species and determine relative contaminations we fitted each peak with a Landau distribution. This hypothesis is justified if high energy particles, were the energy loss fluctuationsin silicon are described by a Landau curve, are selected. This is done requiring energy release variations inside each plane to be below 20% (this selects H above 60 MeV, O above 140 MeV/n, Fe above 250 MeV/n) We have also restricted our analysis to solar quiet days leaving Solar Particle Events to a later work. The data set was divided in three regions according to the McIlwain parameter and the geomagnetic field L: Galactic region ($L > 2$), South Atlantic Anomaly ($L < 2$ and geomagnetic field $B < 0.25$G), and the remaining region ($L < 2,\ B \geq 0.25$ G). In a given point of the orbit the geomagnetic cutoff C determines the minimum energy for primary cosmic rays to reach MIR and to be detected by SilEye. Note that this value refer to particles orthogonal to the local field outside MIR. At $L = 2$, $C = 3.9\ GV$ while at high latitude (L=4.4) $C = 0.8\ GV$. These two values represent the minimum cutoff for a given region; they correspond to a minimum kinetic energy of $\simeq 150\ MeV/n$ ($C = 0.8\ GV$) and $\simeq 1600\ MeV/n$ ($C = 3.9\ GV$). Particles have been selected with the same cut described in the previous subsection. The differences of particle distributions in the three regions are shown in Figure 3. The continuous line shows the galactic component, which has an higher flux of $Z \geq 4$ particles due to the lower geomagnetic cutoff; the wider energy range results in the peaks to be defined less sharply. Proton and helium flux is lower than that measured in the SAA (dotted line) where the trapped component is dominant if compared to galactic and $L < 2$ abundances. Indeed the $L < 2$ curve (dashed) has a lower $Z \leq 2$ flux if compared to SAA but an equal $Z \geq 5$ flux. From these distributions it is possible to reconstruct relative abundances and absolute integral fluxes for different nuclear species (shown respectively in Table 1 and 2. Determination of the proton spectrum requires detailed corrections for the energy dependent trigger efficiency so we currently present only $Z > 4$ results where trigger eficiency can be assumed equal to 1. Note how particle flux (and consequently the dose absorbed by astronauts) varies between regions.

Z	$L > 2$ $(C > 0.6\,GV)$	$L \leq 2$ $(C > 3.9\,GV)$	SAA $(C > 3.9\,GV)$
5 (B)	0.63 ± 0.09	0.53 ± 0.35	0.55 ± 0.09
6 (C)	1 ± 0.1	1 ± 0.06	1 ± 0.12
7 (N)	0.41 ± 0.06	0.34 ± 0.08	0.22 ± 0.04
8 (O)	0.65 ± 0.07	0.66 ± 0.08	0.77 ± 0.17
10 (Ne)	0.33 ± 0.06	0.13 ± 0.02	0.12 ± 0.02
12 (Mg)	0.07 ± 0.02	0.13 ± 0.02	0.12 ± 0.02
14 (Si)	0.05 ± 0.02	0.1 ± 0.02	0.1 ± 0.02

Table 1. Relative abundances normalized to carbon in the three regions (see text).

Z	$L > 2$ $(C > 0.6\,GV)$ $(\times 10^{-5})$ $part/(cm^2\ sr\ s)$	$L \leq 2$ $(C > 3.9\,GV)$ $(\times 10^{-5})$ $part/(cm^2\ sr\ s)$	SAA $(C > 3.9\,GV)$ $(\times 10^{-5})$ $part/(cm^2\ sr\ s)$
5 (B)	(6.6 ± 0.6)	(1.6 ± 1)	(1.5 ± 0.2)
6 (C)	(10.5 ± 0.5)	(3.0 ± 0.1)	(2.6 ± 0.2)
7 (N)	(4.3 ± 0.5)	(1.0 ± 0.2)	(0.59 ± 0.08)
8 (O)	(6.8 ± 0.4)	(2.0 ± 0.2)	(2.0 ± 0.3)
10 (Ne)	(3.5 ± 0.5)	(0.38 ± 0.03)	(0.31 ± 0.06)
12 (Mg)	(0.7 ± 0.2)	(0.39 ± 0.05)	(0.33 ± 0.06)
14 (Si)	(0.5 ± 0.2)	(0.29 ± 0.15)	(0.26 ± 0.05)

Table 2. Integral fluxes above $\simeq 100 MeV/n$ in the three regions

3.1 Linear Energy Transfer

The LET in silicon measured with SilEye-2 is shown in Figure 4: in this work we present solar quiet period data for the three regions described in the previous section. The LET is obtained normalizing the total energy release to the angle of incidence for single and multiple track events. The topmost curve shows the SAA, where trapped protons are the dominant contribution; the galactic nuclear flux (middle curve) is dominant at LET above 8 $keV/\mu m$. The bottom curve represents LET at $L < 2$ and outside the SAA: proton component is below the previous two regions, and the high LET component is - as expected - equal to the SAA region. In these two regions the nuclear component is lower than in the $L > 2$ zone due to the higher geomagnetic cutoff. Trigger efficiency for protons (which constitute the peak at 1 $keV/\mu m$) varies according to incident energy: a detailed Montecarlo simulation, currently in progress, is thus required to reconstruct the original proton spectrum, in order to derive - from the measured LET - the dose absorbed by the cosmonauts.

4 Conclusions

The good behaviour of the SilEye-2 and its particle identification capabilities allow to study the cosmic ray and radiation environment and its short- and long-term temporal variations. Analysis is currently in progress to determine relative abundances and fluxes in these conditions and in presence of Solar Particle Events and to improve the identification capabilities of the device, for instance at low Z and at lower energies. Linear Energy Transfer measurements will be as well used to characterize the radiation environment on board MIR space station in solar quiet and active days.
Two future detectors are planned to continue and extend the observational capabilities of SilEye-2 on the International Space Station: The first , SilEye-3/Alteino, to be launched in 2002 which in addition to new electronics and detectors will also carry an electroencephalograph to perform a real time correlation between Light Flash perceptions by astronaut and cosmic rays. The technology developed for SilEye-3 will be used in the construction of a larger facility, originally proposed in Casolino et al. (1997) and evolved in the Altea (SilEye-4) projectBidoli et al. (1999), currently under development.

References

Avdeev, S. *et al.*, *submitted to Acta Astronautica*.

Bidoli V, Casolino M, De Pascale M, Furano G, Morselli A, Picozza P, Reali E, Sparvoli R, Galper A, Ozerov Yu, Popov A, Zemskov V, Zverev V, Alexandrov A, Avdeev S, Shabelnikov V, Boezio M, Carlson P, Fuglesang C, Barbellini G 1997 *NIM A* **399** 477

Bidoli V, Casolino M, De Pascale M P, Furano G, Morselli A, Narici L, Picozza P, Reali E, Sparvoli R, Galper A, Ozerov Y, Popov A, Vavilov N R, Alexandrov A P, Avdeev S 1999 ESA SP-433

Bidoli V, Casolino M, De Pascale M P, Furano G, Morselli A, Narici L, Picozza P, Reali E, Sparvoli R, Galper A, Ozerov Y, Popov A, Vavilov N R, Alexandrov A P, Avdeev S 2000 *Adv. Space Res.* **10** 2075

Bidoli V, Canestro A, Casolino M, De Pascale M P, Furano G, Iannucci A, Morselli A, Picozza P, Reali E, Sparvoli R, Bakaldin A, Galper A, Koldashov S, Korotkov M, Leonov A, Mikhailov V, Murashov A, Voronov S, Boezio M 2001 *ApJS* **132** 2 365

Casolino M, De Pascale M P, Furano G, Morselli A, Narici L, Picozza P, Reali E, Sparvoli, Adriani O, Spillantini P, Castellini G, Bartalucci S, Catena C, Conti D, Ricci M 1997 *Nuovo Cimento D* **19** 10

Galper A, *et al.* 1996 *Proc. of the Sixth European Symposium on Life Sciences Research in Space* 17-21 June, Trondheim, Norway

Horneck G 1992 *Nucl. Tracks Radiat. Meas.* **20 1** 185

Malachowski M J 1978 LBL Report LBL-5683, National Technical Information Service, Springfield, Virginia

McNulty P J 1996 *IEEE Trans. on Nucl. Sci.* **43 2** 475

Reitz G *et al.* 1996 *Radiat. Meas.* **26** 6 679

Sakaguchi T, Doke T, Hasebe N, Hayashi T, Kashiwagi T, Kikuchi J, Kono S, Nagaoka S, Nakano T, Takagi T, Takahashi K and Takahashi S 1999 *NIM A* **437** 75

Sparvoli R, Bidoli B, Canestro A, Casolino M, DePascale M P, Furano G, Iannucci A, Morselli A, Picozza P, Bakaldin A, Galper A, Koldashov S, Korotkov M, Leonov A, Mikhailov V, Murashov A 2000 *Nuc. Phys. B (proc. Suppl.)* **85** 28

Spillantini P 2000 *Nuc. Pys. B (proc. suppl.)* **85** 3

Tobias C A 1952 *J. Aviat. Med.* **23** 345